

Numerical simulation of tensile failure of concrete using Particle Flow Code (PFC)

Hadi Haeri^{*1} and Vahab Sarfarazi²

¹*Department of Mining Engineering, Bafgh Branch, Islamic Azad University, Bafgh, Iran*

²*Department of Mining Engineering, Hamedan University of Technology, Hamedan, Iran*

(Received March 7, 2016, Revised March 23, 2016, Accepted March 24, 2016)

Abstract. This paper considers the tensile strength of concrete samples in direct, CTT, modified tension, splitting and ring tests using both of the experimental tests and numerical simulation (particle flow code 2D). It determined that which one of indirect tensile strength is close to direct tensile strength. Initially calibration of PFC was undertaken with respect to the data obtained from Brazilian laboratory tests to ensure the conformity of the simulated numerical models response. Furthermore, validation of the simulated models in four introduced tests was also cross checked with the results from experimental tests. By using numerical testing, the failure process was visually observed and failure patterns were watched to be reasonable in accordance with experimental results. Discrete element simulations demonstrated that the macro fractures in models are caused by microscopic tensile breakages on large numbers of bonded discs. Tensile strength of concrete in direct test was less than other tests results. Tensile strength resulted from modified tension test was close to direct test results. So modified tension test can be a proper test for determination of tensile strength of concrete in absence of direct test. Other advantages shown by modified tension tests are: (1) sample preparation is easy and (2) the use of a simple conventional compression press controlled by displacement compared with complicate device in other tests.

Keywords: tensile strength; direct test; CTT test; modified test; splitting test and ring test

1. Introduction

Tensile strength of concrete is of prime importance in case of water retaining structures, runway slabs, pre-stressed concrete members, bond and shear failure of reinforced concrete members and cracking of mass concrete works. Many experimental and theoretical studies have been carried out to determine the tensile strength of concrete (Ayatollahi and Aliha 2008, Janeiro and Einstein 2010, Wang 2010, Dai *et al.* 2010, Yang 2011, Lee and Jeon 2011, Cui *et al.* 2011, Dai *et al.* 2011, Ayatollahi and Sistaninia 2011, Wang *et al.* 2011, Wang *et al.* 2012, Ghazvinian *et al.* 2012, Erarslan and Williams 2012, Cheng-zhi and Ping 2012, Wallin 2013, Wan Ibrahim *et al.* 2015, Tiang *et al.* 2015, Silva *et al.* 2015, Gerges *et al.* 2015, Liu *et al.* 2015, Mobasher *et al.*

*Corresponding author, Assistant professor, E-mail: haerihadi@gmail.com



Fig. 1 Schematic picture of the loading of the specimen in a direct tension test

2014, Kim and Taha 2014, Haeri 2015a, 2015b, 2015c, 2015d, Haeri and Sarfarazi 2016a, Haeri and Marji 2016b, Sarfarazi *et al.* 2016). So far much of the work is done upon the evaluation of tensile strength of concrete by indirect methods and comparatively fewer efforts have been made for its determination by direct methods. However, the tensile strength obtained from the uniaxial tensile test is more reliable than that of other test methods (Fig. 1). But this test method requires much more care compared to indirect methods. Particularly, after the production of strong epoxy based adhesives, the uniaxial tensile tests are done with few troubles. Many experimental researches conducted in the past to determine the uniaxial tensile strength failed because of unexpected crushing which occurred as a result of local stress concentrations. Another difficulty in uniaxial tensile tests is that the test specimen is under the influence of moment effects during the tensile test due to eccentricity. Yerlici (1965) describes that the behavior of concrete under tension has not been extensively investigated because of its limited tensile strength and extensibility.

Split tensile or Brazilian tensile test is indirect method for measuring the tensile strength of concrete. It is accepted since long as it is easy to cast the cylindrical specimen and simple to perform avoiding all complication of axial tension test. For ordinary concrete well known

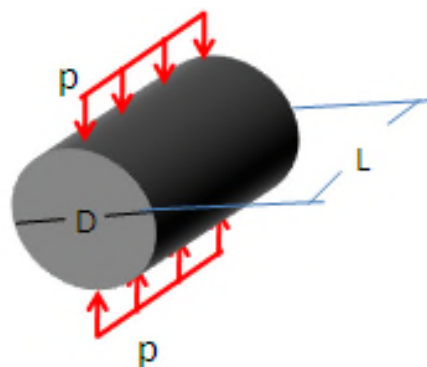


Fig. 2 Schematic picture of the loading of the specimen in a splitting tension test

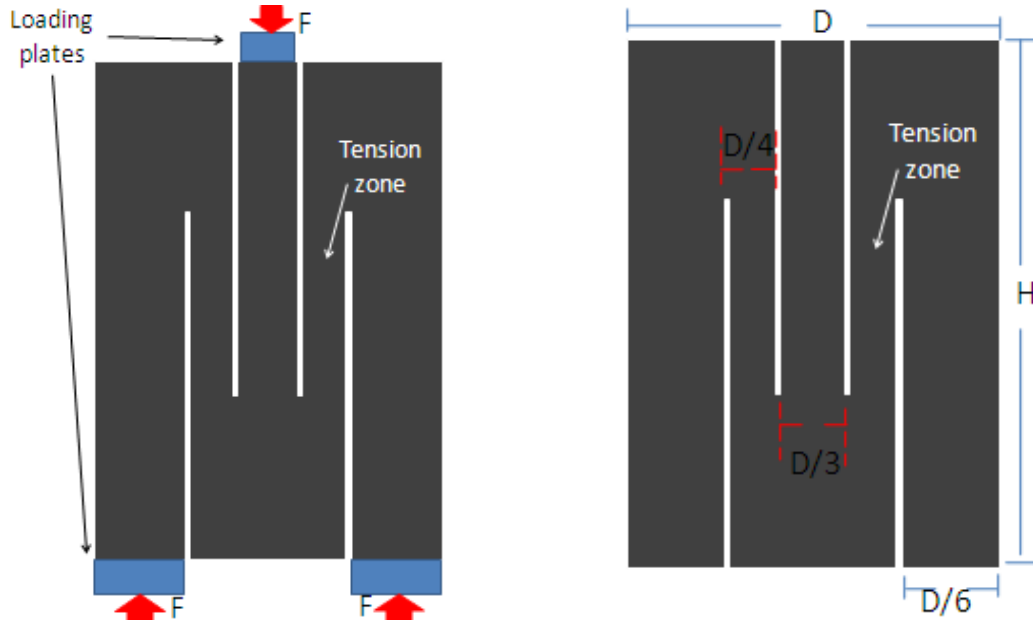


Fig. 3 Model for modified tension test (Blumel 2000)

correlation exists between direct tensile strength and splitting tensile strength. The formula for computing the tensile strength of concrete from the split-cylinder test has been obtained from the theory of linear elasticity (Hannant *et al.* 1973, Tedesco *et al.* 1973, Castro-Montero *et al.* 1995). The measured splitting tensile strength, of the specimen shall be calculated using the following formula

$$\sigma = \frac{2P}{\pi LD} \quad (1)$$

P is maximum load in Newtons applied to the specimen, L is length of the specimen (mm) and d is cross sectional dimension of the specimen (mm) as shown in Fig. 2 (in mm).

Blumel (2000) represents a new and innovative approach to the laboratory research of the uniaxial tensile strength. Fig. 3 shows model for the test features. A cylindrical specimen of special geometry for a unidirectional tensile stress field is created in the sample. The test may easily be carried out in any standard testing machine to test the unconfined tensile strength (UCS).

$$\sigma = \frac{2F}{D} \quad (2)$$

The CTT test proposed by Sarfarazi (2015) is other method for determination of tensile strength of concrete (Fig. 4). A compression to tensile load transforming (CTT) device was developed to determine indirect tensile strength of rock like material. A concrete slab with a hole at its center was prepared and subjected to tensile loading using compression to tension load converter device (Fig. 4). Dimension of specimen and hole diameter were $15 \times 19 \times 6$ cm and 7.5 cm, respectively (Fig. 4). The tensile strength was calculated using following equation

$$\sigma/Pt = 3(W/B) + 1 \quad (3)$$

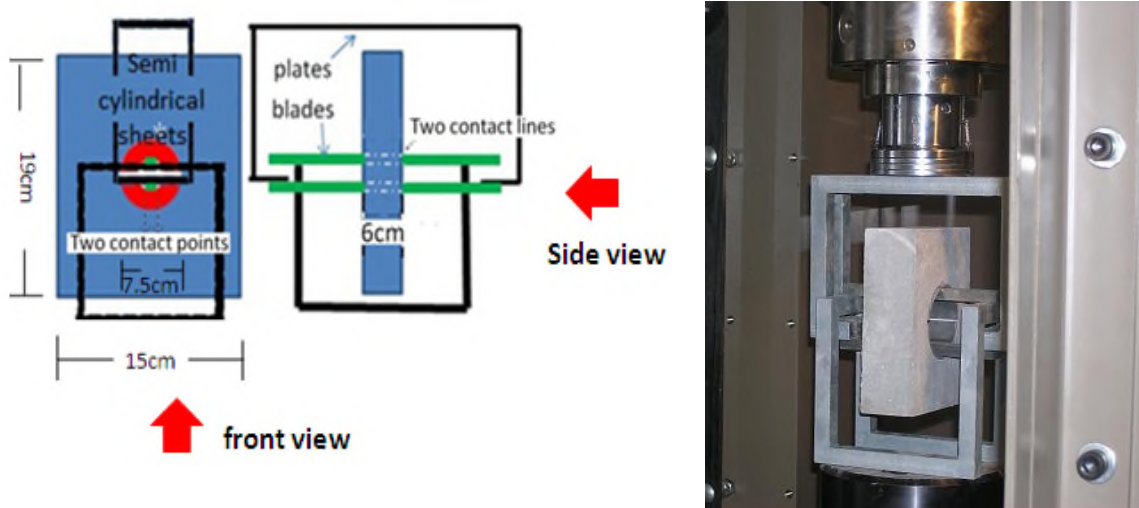


Fig. 4 CTT test (Sarfarazi 2015)

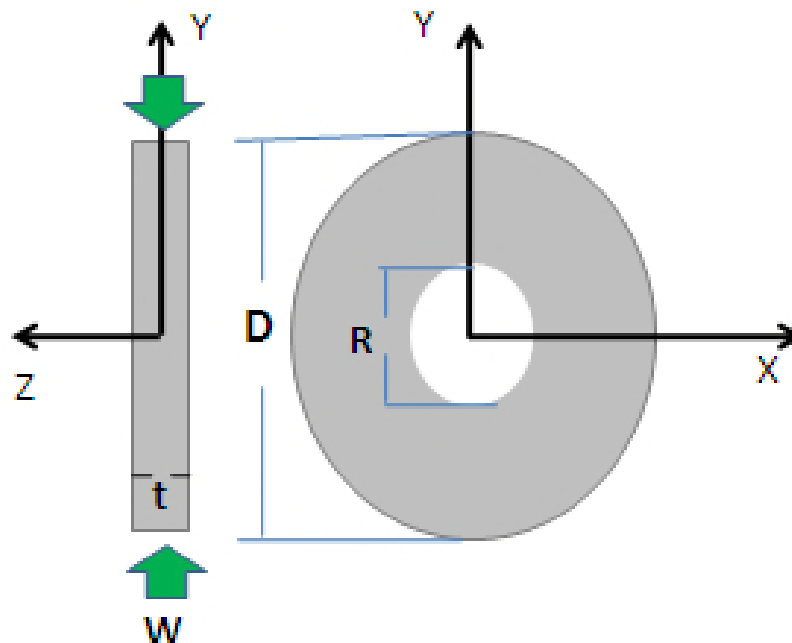


Fig. 5 Ring test (Pandit 1970)

Where σ is tensile strength (MPa), P_t is tensile stress on the CTT test (MPa), W is hole diameter (mm) and B is sample width (mm).

The ring test proposed by Pandit (1970) is other method for determination of tensile strength of concrete (Fig. 5). The ring test has several advantages, such as convenient specimen preparation, simple loading and measurement system, failure starting away from the loading platen, and pure

tensile failure mode. From the previous studies of ring tests, the tensile strength was calculated from the maximum tensile stress occurring at the intersections of vertically loaded diameter and the hole.

Pandit (1970) proposed an approximate solution

$$\sigma = \frac{12W}{\pi Dt} \tag{4}$$

Where, σ is tensile strength, W is the applied line loading; D and t are the external diameter and thickness of the ring.

In this paper, tensile strength of concrete was measured using direct test, flexural test, double punch test and ring test. Experimental tests and particle flow code were used to determine that which one of indirect tensile strength is close to direct tensile strength.

In this paper, tensile strength of concrete has been measured using different numerical methods and the best one was chosen. also the results of numerical simulation were comprised by experimental test results for validation of numerical simulation output.

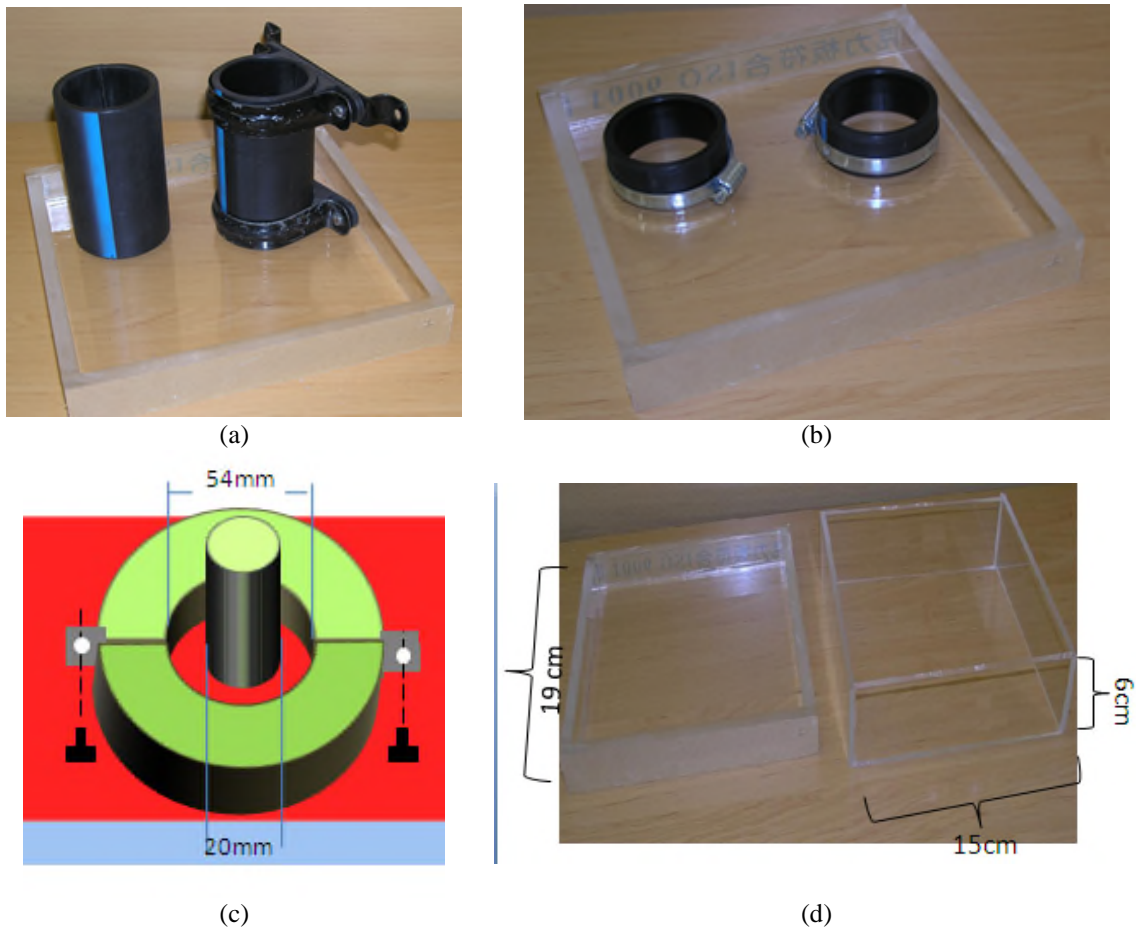


Fig. 6 Different volumes for sampling different types of blocks used in (a) Direct tension test, (b) Brazilian test, (c) CTT test and (d) ring test

2. Experimental tests

2.1 Model material preparation

The concrete specimens were prepared from a mixture of two parts water, one part fine sand, and two parts cement. Mixing, casting and curing of specimens were carefully controlled to obtain reproducible properties. The mixed material was cast in different volumes for sampling different types of blocks (Fig. 6). Diameters for cylindrical and disc samples were set at 54 mm, with the thickness of 108 mm and 27 mm, respectively (Fig. 6(a), (b)). Dimensions of CTT test sample were 190mm×150mm×60mm. diameter of sample's hole was 7.5 cm (Fig. 6(c)). Diameters of ring samples were set at 54 mm (Fig. 6(d)). Samples kept in geo-mechanics laboratory room for 20 days at 20 ± 2 °C before being subjected to mechanical testing. Uniaxial tension test, Brazilian tensile tests, CTT test, Blumel test and ring test were performed for determining the tensile strength and failure mode of intact model material.

3. Particle flow code

In simulation of bonded particle model by PFC2D, rock material is represented as an assembly of circular disks bonded together at their contact points and confined by planar walls. The particles are bonded together at their contacts to simulate a competent rock. There are two basic bonding models supported in PFC: a contact –bonded model and a parallel-bonded model. A contact bond approximates the physical behavior of a vanishingly small cement-like substance lying between and joining the two bonded particles. The contact bond behaves as a parallel bond of radius zero. Thus, a contact bond does not have a radius or shear and normal stiffness as does a parallel bond, and can not resist a bending moment; rather, it can only resist force acting at the contact point. The contacts bonds are assigned with specified tensile and shear strength which allows resistance to tension and shear to exist at the contacts until the force at the contact exceeds the strength of the bond. The mechanics of PFC are described in detail in (Cundall and Strack, 1979; Itasca, 2003) and will not be repeated here. In order to generate a contact bonded particle model for PFC2D, using the routines provided in (Cundall and Strack, 1979), the following micro parameters should be defined: Ball-to-ball Contact Modulus, stiffness ratio KN over KS, ball friction coefficient, contact Normal Bond Strength, contact Shear Bond Strength, Ratio of Standard Deviation to mean of bond strength both in normal and shear direction, and minimum Ball radius. Defining a parallel-bonded particle model requires three additional micro parameters, which are: parallel-bond radius multiplier, parallel-bond modulus, and parallel-bond stiffness ratio. In this study, bonded particle models are created by assuming that particles are joined and bonded together using the parallel bonded model. Whereas PFC2D was used for simulation work, the thickness of model is equal to unite and plane strain condition was established in the model.

3.1 Splitting or Brazilian test

Brazilian test was used to calibrate the tensile strength of specimen in PFC2D model. Adopting the micro-properties listed in Table 1 and the standard calibration procedures (Potyondy and Cundall 2004), a calibrated PFC particle assembly was created. The diameter of the Brazilian disk considered in the numerical tests was 54 mm (Fig. 7(a)). The specimen was made of 5,615

Table 1 Micro properties used to represent the concrete

Parameter	Value	Parameter	Value
Type of particle	disc	Parallel bond radius multiplier	1
density	1000	Young modulus of parallel bond (GPa)	40
Minimum radius	0.27	Parallel bond stiffness ratio	1.7
Size ratio	1.56	Particle friction coefficient	0.4
Porosity ratio	0.08	Parallel bond normal strength, mean (MPa)	25
Damping coefficient	0.7	Parallel bond normal strength, SD (MPa)	2
Contact young modulus (GPa)	40	Parallel bond shear strength, mean (MPa)	25
Stiffness ratio	1.7	Parallel bond shear strength, SD (MPa)	2

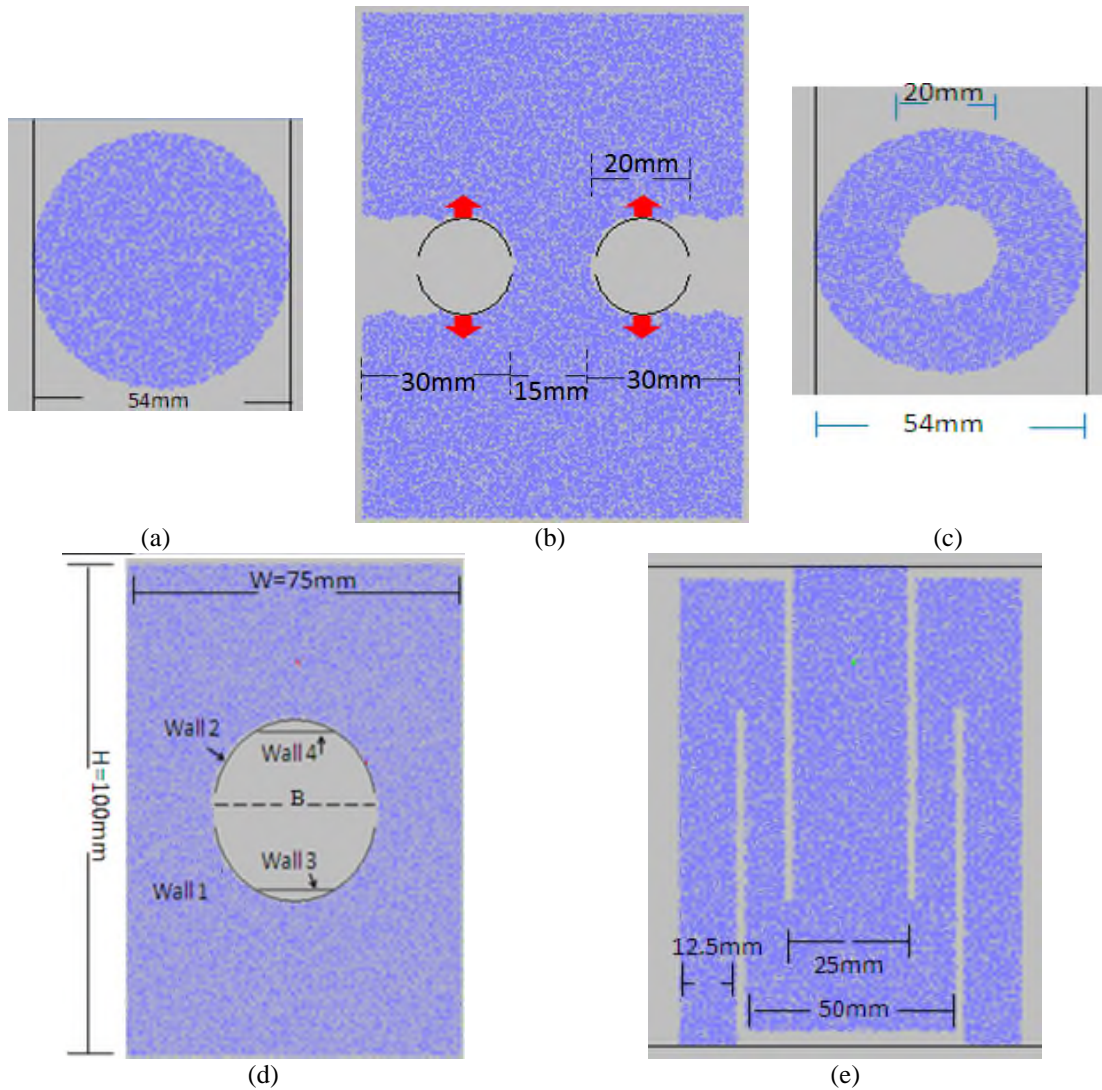


Fig. 7 Specification of numerical model, (a) direct tensile test, (b) Brazilian test, (c) ring test, (d) CTT test and (e) modified tension test

particles. The disk was crushed by the lateral walls moved toward each other with a low speed of 0.016 m/s. The wall velocity was adequate low (0.016 m/s in all tests) to ensure a quasi-static equilibrium. According to the paper published by Sarfarazi *et al.* (2012), the wall velocity of 0.16 m/s was adequate low to ensure a quasi-static equilibrium.

Its to be note that according to Itasca manual, the porosity of models was equal to 0.08. This value was appropriated for calibration of model. Also this value was different from real porosity of physical samples.

3.2 Direct tensile test

After calibration of PFC2D, direct tensile tests were simulated by creating a box model in the PFC2D (by using the calibrated micro-parameters) (Fig. 7(b)). The PFC specimen had the dimensions of 75 mm×100 mm. A total of 11,179 disks with a minimum radius of 0.27 mm were used to make up the shear box specimen. Two rectangular zones with length of 30 mm and thickness of 20 mm, was removed from the right and left sides of the model. After model preparation, four semi circle loading wall were installed in contact with the hole wall (Fig. 7(b)). Tensile loading was applied to the sample by moving the upper and lower walls in the positive side of Y-direction and in the opposite side of Y-direction, respectively. The Tensile force was registered by taking the reaction forces on the wall 3 in Fig. 7(b).

3.3 Ring test

Ring test was simulated by creating a circle model in the PFC2D (by using the calibrated micro-parameters) (Fig. 7(c)). Diameter of the Ring disk was 54 mm. a circle with diameter of 20 mm was removed from the model. The specimen was made of 4312 particles. The disk was crushed by the lateral walls moved toward each other. The Tensile force was registered by taking the reaction forces on the wall 1 in Fig. 7(c).

3.4 CTT test

CTT test was simulated by creating a box model in the PFC2D (Fig. 7(d)). The PFC specimen had the dimensions of 75*100 mm. A total of 11,179 disks with a minimum radius of 0.27 mm were used to make up the shear box specimen. A hole with diameter of B was formed in the middle of model by deletion of particles from it. After model preparation, two semi circle loading wall (walls 1 and 2) were installed in contact with the hole wall (Fig. 7(d)). Also two horizontal walls (walls 3 and 4) with 2cm of width were situated in contact with the semi circle walls (Fig. 7(d)). Tensile loading was applied to the sample by moving the upper and lower walls in the positive side of Y-direction and in the opposite side of Y-direction, respectively. The Tensile force was registered by taking the reaction forces on the wall 3 in Fig. 7(d).

3.5 Modified tension test

Modified tension test was simulated by creating a box model in the PFC2D (by using the calibrated micro-parameters) (Fig. 7(e)). The PFC specimen had dimensions of 100 mm×75 mm. For forming the joints, four vertical bands with thickness of 3 mm were removed from the model. Horizontal distance between outer bands is 50 mm and horizontal distance between inner bands is

25 mm. Also, for creating the test condition, three horizontal bands with thickness of 3 mm were removed from top and bottom of the model (Fig. 7(e)). A total of 10012 disks with a minimum radius of 0.27 mm were used. After model preparation, two loading wall were installed in the top and bottom the model. Tensile loading was applied to the sample by moving the lower and upper walls in the positive side of Y-direction and in the opposite side of Y-direction, respectively. The Tensile force was registered by taking the reaction forces on the wall 1 in Fig. 7(e).

4. Tensile failure mechanism

4.1 Comparison between failure patterns in numerical models and experimental samples

Figs. 8-12 shows progress of cracks in direct test, modified tension test, CTT test, splitting test and ring test respectively. In each figure, the results of numerical simulation and experimental test have been shown. Black lines and red lines represent the tensile cracks and shear cracks, respectively. Fig. 8(a) shows that under direct test, the model gets broken from the middle with diagonal tensile cracks what happens in experimental test (Fig. 8(b)).

Fig. 9(a) shows that under modified tension test, bridges gets broken by two horizontal tensile fractures.

Fig. 10(a) shows that under CTT test, model cracked along a horizontal line through the center of the hole. The model gets broken from the middle by two horizontal tensile fractures what happens in experimental test (Fig. 10(b)).

Fig. 11(a) shows that under splitting test, model cracked along a vertical line through the center of the model. The model gets broken from the middle. The failure planes experienced in numerical and laboratory tests are well matching (Fig. 11(b)).

Fig. 12(a) shows that under ring test, model gets broken by one horizontal tensile fracture what happens in experimental test (Fig. 12(b)).

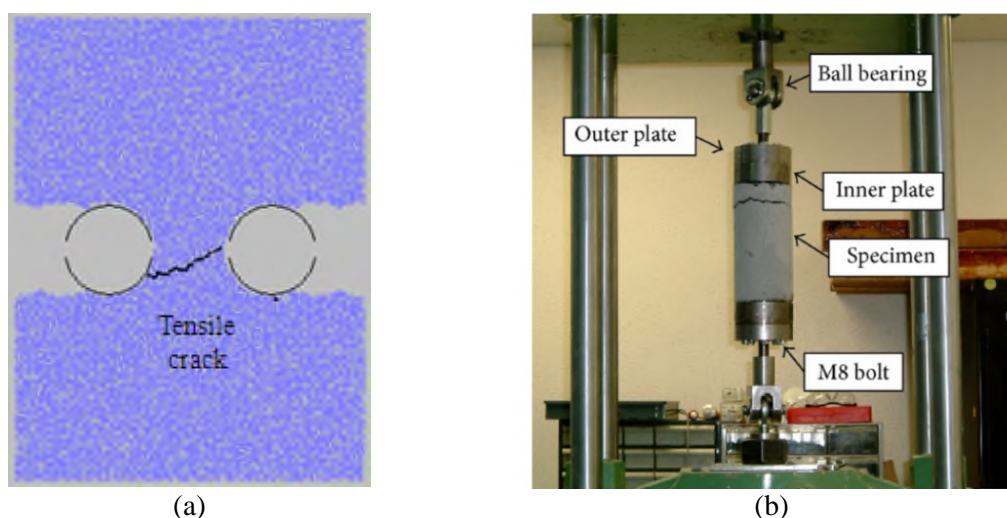


Fig. 8 Failure pattern in direct test, a) numerical simulation, b) experimental test

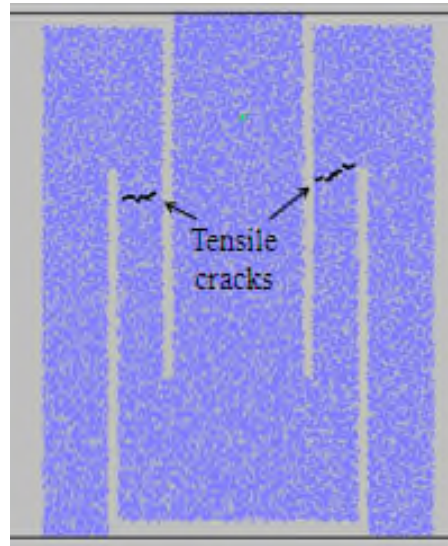
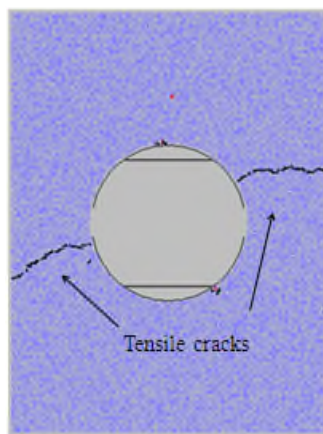
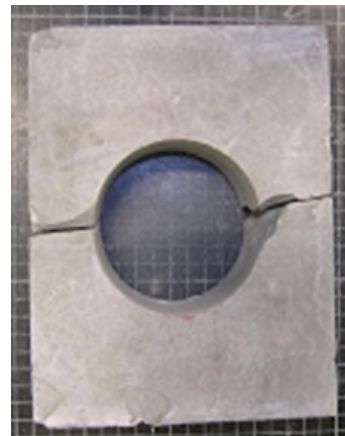


Fig. 9 Numerical failure pattern in modified tension test

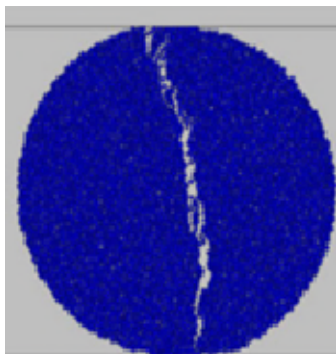


(a)

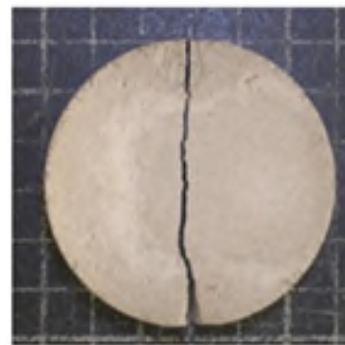


(b)

Fig. 10 Failure pattern in CTT test, (a) numerical simulation, (b) experimental test



(a)



(b)

Fig. 11 Failure pattern in Splitting test, (a) numerical simulation, (b) experimental test

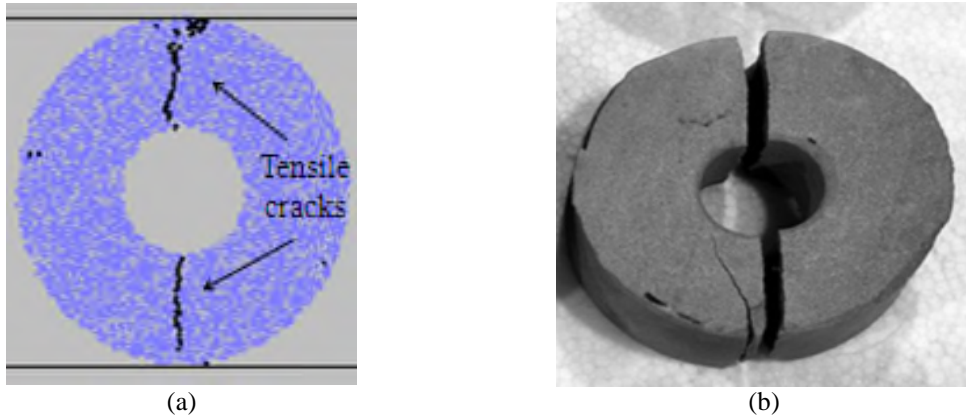


Fig. 12 Failure pattern in ring test, a) numerical simulation, b) experimental test

Table 2 Results of direct test and punch test flexural test and ring test

Tensile strengths	direct test	CTT test	Modified tension test	Splitting test	tring test
Tensile strength in numerical simulation (MPa)	4	4.4	4	4.6	13.5
Tensile strength in experimental test (MPa)	3.7	4.2		4.5	9

4.2 Comparison between tensile strength in numerical models and experimental samples

Table 2 shows a comparison between the tensile strengths for direct test, CTT test, Modified tension test, Splitting test and ring test in both of the numerical and experimental tests.

Results from numerical and experimental tests show that, tensile strength obtained from experimental tests were less than numerical one. This is due to the presence of micro cracks and micro pore in the physical samples which lead to lower tensile strength. Direct tension test and modified tension test yield the lowest strength values (Table 2) due to high tensile stress distribution on failure surface. Tensile strength obtained by these two methods is 4 MPa. Ring test yields the highest strength values in both of numerical and experimental test (Table 2). The difference between numerical CTT test, Splitting test and ring test related to direct tensile strengths is about 10%, 15% and 237.5%. It is interesting to note that tensile strength obtained by flexural test was near to the direct tensile strength. So modified tension test can be a proper test for determination of tensile strength of concrete in absence of direct test. Other advantages shown by punch tests are: (1) the modified tension test is easy for sample preparation, (2) the use of a simple conventional compression press controlled by displacement compared with complicate device in other tests.

5. Discussions and conclusions

The tensile failure behavior of concrete in indirect tests (CTT test, modified tension test, splitting test and ring tests) and direct test has been investigated using experimental test and numerical simulations.

By using numerical testing, the failure process was visually observed and failure patterns were watched to be reasonable in accordance with experimental results. Discrete element simulations demonstrated that the macro fractures in models are caused by microscopic tensile breakages on large numbers of bonded discs. Tensile strength of concrete in direct test was less than other tests results. Tensile strength resulted from modified tension test was close to direct test results. So modified tension test can be a proper test for determination of tensile strength of concrete in absence of direct test. Other advantages shown by punch tests are: (1) sample preparation is easy in modified tension test, (2) the use of a simple conventional compression press controlled by displacement compared with complicate device in other tests.

References

- Ayatollahi, M.R. and Aliha, M.R. (2008), "On the use of Brazilian disc specimen for calculating mixed mode I-II fracture toughness of rock materials", *Eng. Fract. Mech.* **75**(16), 4631-4641.
- Ayatollahi, M.R. and Sistaninia, M. (2011), "Mode II fracture study of rocks using Brazilian disk specimens", *Int. J. Rock Mech. Min. Sci.*, **48**(5), 819-826.
- Blumel, M. (2000), "Improved procedures for laboratory rock testing", *Proceedings of the EUROCK 2000 Symposium*, Aachen, Essen, 573-578.
- Castro-Montero, A., Jia, Z. and Shah, S.P. (1995), "Evaluation of damage in brazilian test using holographic interferometry", *ACI Mater. J.*, **92**(3), 268-275.
- Cheng-zhi, P. and Ping, C. (2012), "Breakage characteristics and its influencing factors of rock-like material with multi-fissures under uniaxial compression", *Trans. Nonferrous Met. Soc. China.*, **22**(1), 185-191.
- Cui, M., Zhay, Y. and Ji, G. (2011), "Experimental study of rock breaking effect of steel particles", *J. Hydrodyn.*, **23**(2), 241-246.
- Cundall, P.A. and Strack, O.D.L. (1979), "A discrete numerical model for granular assemblies", *Geotechnique*; **29**(1), 47-65.
- Dai, F., Chen, R., Iqbal, M.J. and Xia, K. (2010), "Dynamic cracked chevron notched Brazilian disc method for measuring rock fracture parameters", *Int. J. Rock Mech. Min. Sci.*, **47**(4), 606-613.
- Dai, F., Xia, K., Zheng, H. and Wang, Y.X. (2011), "Determination of dynamic rock mode-I fracture parameters using cracked chevron notched semi-circular bend specimen", *Eng. Fract. Mech.*, **78**(15), 2633-2644.
- Erarslan, N. and Williams, D.J. (2012), "The damage mechanism of rock fatigue and its relationship to the fracture toughness of rocks", *Int. J. Rock Mech. Min. Sci.*, **56**, 15-26.
- Gerges, N., Issa, C. and Fawaz, S. (2015), "Effect of construction joints on the splitting tensile strength of concrete", *Case Studies in Constr. Mater.*, **3**, 83-91.
- Ghazvinian, A, Nejati, H.R., Sarfarazi, V. and Hadei, M.R. (2012), "Mixed mode crack propagation in low brittle rock-like materials", *Arab. J. Geosci.*, **6**(11), 4435-4444.
- Haeri, H. (2015a), "Influence of the inclined edge notches on the shear-fracture behavior in edge-notched beam specimens", *Comput. Concrete* , **16**(4), 605-623,
- Haeri, H. (2015b), "Experimental crack analysis of rock-like CSCBD specimens using a higher order DDM", *Comput. Concrete*, **16**(6), 881-896.
- Haeri, H. (2015c), "Simulating the crack propagation mechanism of pre-cracked concrete specimens under Shear Loading Conditions", *Strength Mater.*, **47**(4), 618-632.
- Haeri, H. (2015d), "Propagation mechanism of neighboring cracks in rock-like cylindrical specimens under uniaxial compression", *J. Min. Sci.*, **51**(3), 487-496.
- Haeri, H. and Marji, M.F. (2016b), "Simulating the crack propagation and cracks coalescence underneath TBM disc cutters", *Arab. J. Geo.*, **9**(2), 1-10.
- Haeri, H. and Sarfarazi, V., (2016a), The effect of micro pore on the characteristics of crack tip plastic zone in concrete, *Computers and Concrete*, **17**(1), 107-12.

- Hannant, D.J., Buckley, K.J. and Croft, J. (1973), "The effect of aggregate size on the use of the cylinder splitting test as a measure of tensile strength", *Matér. Constr.*, **6**(1), 15-21.
- Ibrahim, M.W., Hamzah, A.F., Jamaluddin, N., Ramadhansyah, P.J. and Fadzil, A.M. (2015), "Split tensile strength on self-compacting concrete containing coal bottom ash", *Procedia-Social and Behavioral Sciences*, **195**, 2280-2289.
- Itasca Consulting Group Inc. (2003), "PFC3D (particle flow code in 3dimensions) version 3.0". Minneapolis: Itasca.
- Janeiro, R.P. and Einstein, H.H. (2010), "Experimental study of the cracking behavior of specimens containing inclusions (under uniaxial compression)", *Int. J. Fract.*, **164**(1), 83-102.
- Kim, J.J. and Reda Taha, M. (2014), "Experimental and numerical evaluation of direct tension test for cylindrical concrete specimens", *Adv. Civil Eng.*, 1-8.
- Liu, X., Nie, Z., Wu, S. and Wang, C. (2015), "Self-monitoring application of conductive asphalt concrete under indirect tensile deformation", *Case Studies Constr. Mater.*, **3**, 70-77.
- Mobasher, B., Bakhshi, M. and Barsby, C. (2014), "Backcalculation of residual tensile strength of regular and high performance fiber reinforced concrete from flexural tests", *Constr. Build. Mater.*, **70**, 243-253.
- Pandit, G.S. (1970), "Concrete rings for determining tensile strength of concrete", *ACI J.*, 847-848.
- Potyondy, D.O. and Cundall, P.A. (2004), "A bonded-particle model for rock", *Int. J. Rock Mech. Min. Sci.*, **41**(8), 1329-1364.
- Sarfarazi, V., Ghazvinian, A., Schubert, W., Blumel, M. and Nejati, H.R. (2014), "Numerical simulation of the process of fracture of echelon rock joints", *Rock Mech. Rock Eng.*, **47**(4), 1355-1371.
- Sarfarazi, V. (2015), "A new approach for measurement of tensile strength of concrete, the first international and the thired national conference of architecture", *Constr. Urban Envir.*, 1-8.
- Sarfarazi, V., Hamid R.F., Haeri, H. and Wulf, S. (2016), "A new approach for measurement of anisotropic tensile strength of concrete", *Adv. Concrete Constr.*, **3**(4), 269-286.
- Silva, R.V., Brito, J. and Dhir, R.K. (2015), "Tensile strength behaviour of recycled aggregate concrete", *Constr. Build. Mater.*, **83**, 108-118.
- Tedesco, J.W. and Ross, C.A. and Kuennen, S.T. (1973), "Experimental and numerical analysis of high strain rate splitting tensile tests", *ACI Mater. J.*, **90**, 162-169.
- Tiang, Y., Shi, S., Jia, K. and Hu, S. (2015), "Mechanical and dynamic properties of high strength concrete modified with lightweight aggregates presaturated polymer emulsion", *Constr. Build. Mater.*, **93**, 1151-1156.
- Wallin, K. (2013), "A simple fracture mechanical interpretation of size effects in concrete fracture toughness tests", *Eng. Fract. Mech.*, **99**, 18-29.
- Wang, Q.Z. (2010), "Formula for calculating the critical stress intensity factor in rock fracture toughness tests using cracked chevron notched Brazilian disc (CCNBD) specimens", *Int. J. Rock Mech. Min. Sci.*, **47**(6), 1006-1011.
- Wang, Q.Z., Feng, F., Ni, M. and Gou, X.P. (2011), "Measurement of mode I and mode II rock dynamic fracture toughness with cracked straight through flattened Brazilian disc impacted by split Hopkinson pressure bar", *Eng. Fract. Mech.*, **78**(12), 2455-2469.
- Wang, Q.Z., Gou, X.P. and Fan, H. (2012), "The minimum dimensionless stress intensity factor and its upper bound for CCNBD fracture toughness specimen analyzed with straight through crack assumption", *Eng. Fract. Mech.*, **82**, 1-8.
- Yang, S.Q. (2011), "Crack coalescence behavior of brittle sandstone samples containing two coplanar fissures in the process of deformation breakage", *Eng. Fract. Mech.*, **78**, 3059-3081.
- Yerlici, Vedat A. (1965), "Behavior of plain concrete under axial tension", *ACI J.*, 987.

